

Chiral skyrmions of large radius

Stavros Komineas

Department of Mathematics and Applied Mathematics, University of Crete, 70013 Heraklion, Crete, Greece

Christof Melcher

Department of Mathematics & JARA Fundamentals of Future Information Technology, RWTH Aachen University, 52056 Aachen, Germany

Stephanos Venakides

Department of Mathematics, Duke University, Durham, NC, USA

Abstract

We study the structure of an axially symmetric magnetic skyrmion in a ferromagnet with the Dzyaloshinskii-Moriya interaction. We examine the regime of large skyrmions and we identify rigorously the critical value of the dimensionless parameter at which the skyrmion radius diverges to infinity, while the skyrmion energy converges to zero. This critical value coincides with the expected transition point from the uniform phase, which accommodates the skyrmion as an excited state, to the helical phase, which has negative energy. We give the profile field at the skyrmion core, its outer field, and the intermediate field at the skyrmion domain wall. Moreover, we derive an explicit formula for the leading asymptotic behavior of the energy as well as the leading term and first asymptotic correction for the value of the critical parameter. The key leading to the results is a parity theorem that utilizes exact formulae for the asymptotic behavior of the solutions of the static Landau-Lifshitz equation centered at the skyrmion domain wall. The skyrmion energy is shown to be an odd function of the radius and the dimensionless parameter to be an even function.

Keywords: Magnetic skyrmion, Micromagnetics, Dzyaloshinskii-Moriya interaction

2000 MSC: 49S05: Variational principles of physics, 35Q51: Solitons, 82D40: Magnetic materials,

34B15: Nonlinear boundary value problems

1. Introduction

Magnetic skyrmions are two-dimensional topological solitons in the magnetization field $\mathbf{m} : \mathbb{R}^2 \cup \{\infty\} \rightarrow \mathbb{S}^2$ with $\deg \mathbf{m} = \pm 1$. After their theoretical prediction [1, 2] they have been observed in ferromagnets with the Dzyaloshinskii-Moriya (DM) interaction and techniques have been developed for individual skyrmions to be created and annihilated in a controlled manner [3, 4, 5, 6]. DM interaction arises from the loss of chiral symmetry induced by the underlying crystal structure or due to thin-film or multilayer geometries. Chiral interaction terms and chiral skyrmions also arise in variational models for other condensed matter systems including spin-orbit coupled Bose-Einstein condensates (BEC) [7, 8] or nematic liquid crystals [9, 10].

Our model is based on a micromagnetic energy functional that includes exchange, DM and easy-axis anisotropy terms. The system can be described by a single dimensionless DM parameter ϵ , defined in Eq. (3), given as the ratio of the DM parameter divided by (half) the domain wall energy. It is known (though not rigorously proven yet) that, there are only two phases minimizing the energy per unit area: the

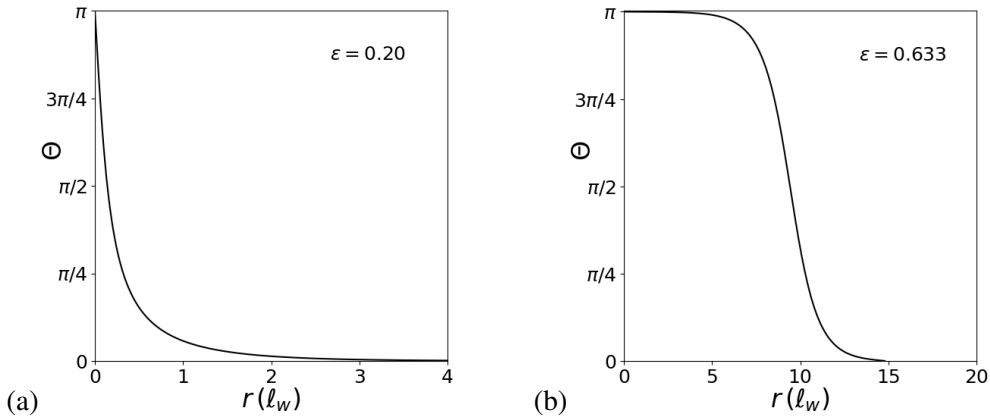


Figure 1: In contrast to the small skyrmion (a) being a localized perturbation of the Belavin-Polyakov soliton, the key feature of the large skyrmion (b) is a domain wall structure that separates the core from the far field. The slope of the profile approaches π exponentially in the limit of large radius.

uniform phase and the helical phase for small and for large DM parameter ϵ respectively [2]. The spiral state has negative energy. The transition from the spiral to the uniform state is achieved as the period of the spiral goes to infinity for $\epsilon \rightarrow 2/\pi$.

The isolated chiral skyrmion is an excited state in the parameter regime of non-negative energy where the uniform state is the absolute energy minimizer. Most approaches are based on the assumption of axial symmetry so that \mathbf{m} is represented by its polar angle $\Theta = \Theta(r)$ depending on the radial coordinate $r > 0$. The existence of skyrmionic solutions as local minimizers of the micromagnetic energy has been rigorously proven for the case of an external field [11, 12]. The argument has been extended to the case of uniaxial anisotropy including stray-field interaction [13, 14], and to director models of chiral liquid crystals [15].

Skyrmionic solutions of the static Landau-Lifshitz equation in the presence of a DM term can be found by numerical methods [2, 16]. Numerical results provide the phase diagram for the existence of skyrmions and various features of the skyrmion profile. Skyrmions exhibit different morphologies depending on the value of ϵ , see Figure 1. For skyrmions of large radius, an ad-hoc ansatz based on explicit (1D) domain wall profiles [17] has been suggested and is widely used to examine structural and dynamic properties, see, e.g., [18, 19, 20]. In Ref. [21] a 1D profile with the domain wall width as an additional parameter is used. In recent years, sufficient resolution has been obtained for the observation of the features of the skyrmion profile in great detail [18, 22, 16, 23, 24, 25, 26]. The skyrmion profile determines to a large extent, and sometimes crucially, the skyrmion properties [27]. The profile enters in formulae for dynamical phenomena, for example, skyrmion translation and oscillation modes [21, 28] or antiferromagnetic skyrmion excitations [29], and it is crucial for quantitative calculations. The availability of a detailed analytical description of the skyrmion profile is thus important and it will open the way for a wider exploitation of individual skyrmions.

For the case of skyrmions of small radius, analytic formulae for the profile of axisymmetric skyrmions have been derived [30]. In this asymptotic regime where the dimensionless DM parameter ϵ is small, magnetic skyrmions are well approximated on small scales by the classical Belavin-Polyakov soliton. The results in Ref. [30] provide a quantitative description of this approximation in terms of asymptotic formulae for the skyrmion radius $R \sim \frac{\epsilon}{|\ln \epsilon|}$ and energy $E - 4\pi \sim \frac{\epsilon^2}{\ln \epsilon}$ for $\epsilon \ll 1$ and is underpinned by numerical calculations. Logarithmic scaling has been predicted earlier by using a simplified skyrmion profile [31].

This study provides a derivation of formulae for the skyrmion profile in the large radius limit. Three

series represent the profiles of the core, of the domain wall and of the far field, respectively. The series for the core and the far field are obtained as Modified Bessel functions. The bulk of this work is in the derivation of the domain wall profile, represented as an asymptotic series in negative powers of the skyrmion radius R , which plays the role of the asymptotic parameter. The series covering the domain wall is matched with the core series on the one side and with the far field series on the other side. The matching occurs in overlap regions on either side of the domain wall. The matching of the series is facilitated by an interesting parity symmetry that is exhibited by the series for the domain wall and is mirrored on the series on either side. As a result, the skyrmion profile is represented over the full spatial extent.

Our analysis predicts a breakdown of skyrmion solutions, via a diverging radius, when approaching the threshold value $\epsilon = 2/\pi$ from below, and thereby supports its role as critical constant. The scaled DM parameter ϵ is provided in the form of an even asymptotic series in powers of inverse R . Finally, the analysis determines that the skyrmion energy is expressed as an odd asymptotic series in inverse powers of R . The energy goes to zero as the skyrmion radius goes to infinity.

The results of the present analysis for large radius, taken in combination with the results of Ref. [30] for small radius give a reasonably complete description of the skyrmion profile and of the energy dependence on ϵ .

The paper is organized as follows. In Sec. 2 we explain the mathematical model and present the equation for the skyrmion profile. In Sec. 3 we give a systematic method to obtain an asymptotic series for the skyrmion profile at the domain wall and the relation between the skyrmion radius R and the DM parameter ϵ . In Sec. 4, we give formulae for the skyrmion profile in the core and the far field. Sec. 5 obtains asymptotic matching on overlap region on either side of the domain wall. It also contains further formulae for the core and the far field. In Sec. 6, we apply the theory of Sec. 3 and obtain numerical values for the quantities in the asymptotic formulae. Sec. 7 gives an asymptotic expansion for the skyrmion energy. Sec. 8 contains our concluding remarks. Appendix A contains the proof of a theorem which establishes a fundamental parity property for the skyrmion profile that forces the matching of the series in the domain wall with the series of the core and of the far field. Appendix B contains the details of calculations used in the main text.

2. The skyrmion equation

We consider a two-dimensional ferromagnet on the xy -plane with exchange, Dzyaloshinskii-Moriya interaction, and anisotropy of the easy-axis type perpendicular to the plane. The micromagnetic structure is described via the magnetization vector $\mathbf{m} = \mathbf{m}(x, y)$ with a fixed magnitude normalized to unity, $m^2 = 1$. The normalized form of the micromagnetic energy reads [30]

$$E_\epsilon(\mathbf{m}) = \int \left[\frac{1}{2} \partial_\mu \mathbf{m} \cdot \partial_\mu \mathbf{m} + \frac{1}{2} (1 - m_3^2) + \epsilon e_{\text{DM}} \right] dx. \quad (1)$$

A summation over repeated indices $\mu = 1, 2$ is assumed. The last term in the parenthesis in Eq. (1) models the DM interaction. Prototypical cases are the bulk DM interaction form $e_{\text{DM}} = \hat{\mathbf{e}}_\mu \cdot (\partial_\mu \mathbf{m} \times \mathbf{m})$ and the interfacial DM interaction form $e_{\text{DM}} = \epsilon_{\mu\nu} \hat{\mathbf{e}}_\mu \cdot (\partial_\nu \mathbf{m} \times \mathbf{m})$, where $\epsilon_{\mu\nu}$ is the totally antisymmetric two-dimensional tensor. Here $\hat{\mathbf{e}}_1, \hat{\mathbf{e}}_2, \hat{\mathbf{e}}_3$ are the unit vectors for the magnetization in the respective directions. Static magnetization configurations satisfy the static Landau-Lifshitz equation

$$\mathbf{m} \times (\partial_\mu \partial_\mu \mathbf{m} + m_3 \hat{\mathbf{e}}_3 - 2\epsilon \mathbf{h}_{\text{DM}}) = 0. \quad (2)$$

where the last term is the DM field with $\mathbf{h}_{\text{DM}} = \hat{\mathbf{e}}_\mu \times \partial_\mu \mathbf{m}$ in case of bulk interaction or $\mathbf{h}_{\text{DM}} = \epsilon_{\mu\nu} \hat{\mathbf{e}}_\mu \times \partial_\nu \mathbf{m}$ in case of interfacial DM. In Eq. (1) and (2), lengths are measured in units of the domain wall width

$\ell_w = \sqrt{A/K}$, where A is the exchange and K the anisotropy constant. The equation contains a single parameter

$$\epsilon = \frac{\ell_S}{\ell_w} = \frac{D}{2\sqrt{AK}} \quad (3)$$

defined via an additional length scale of this model $\ell_S = D/(2K)$, where D is the DM parameter (in Ref. [2], a parameter which differs from ϵ only by a constant factor has been introduced). We will refer to ϵ as the *dimensionless DM parameter*, but one should keep in mind that it can also be controlled by changing the anisotropy or the exchange parameter. The lowest energy (ground) state is the spiral for $\epsilon > 2/\pi$ and the ferromagnetic state for $\epsilon < 2/\pi$ [2].

Let us consider the angles (Θ, Φ) for the spherical parametrization of the magnetization vector, and the polar coordinates (r, ϕ) for the film plane. We assume an axially symmetric skyrmion with $\Phi = \phi + \phi_0$ and $\Theta = \Theta(r)$. For a bulk DM term the energy is minimized for $\phi_0 = \pi/2$ (Bloch skyrmion) and for interfacial DM interaction we choose $\phi_0 = 0$ (Néel skyrmion). A value $0 < \phi_0 < \pi/2$ should be chosen if the DM term is a combination of the bulk and interfacial terms.

The skyrmion profile arises as a local minimizer of the energy

$$E_\epsilon(\mathbf{m}) = 2\pi \int_0^\infty \left[\frac{1}{2} \left(\frac{d\Theta}{dr} \right)^2 + \frac{1}{2} \left(1 + \frac{1}{r^2} \right) \sin^2 \Theta + \epsilon \left(\frac{d\Theta}{dr} + \frac{1}{2r} \sin 2\Theta \right) \right] r dr \quad (4)$$

of

$$\mathbf{m}(r, \phi) = (\sin \Theta \cos(\phi + \phi_0), \sin \Theta \sin(\phi + \phi_0), \cos \Theta)$$

whereby $\Theta = \Theta(r)$ satisfies the equation

$$\Theta'' + \frac{\Theta'}{r} - \frac{\sin(2\Theta)}{2r^2} - \frac{\sin(2\Theta)}{2} + 2\epsilon \frac{\sin^2 \Theta}{r} = 0 \quad (5)$$

with boundary conditions $\Theta(0) = \pi$ and $\lim_{r \rightarrow \infty} \Theta(r) = 0$. The same equation applies to all types of skyrmions, e.g., Bloch and Néel skyrmions for the respective DM terms.

3. High order analysis of the skyrmion domain wall

We study skyrmions with large radius R , defined by the equation

$$\Theta(R) = \frac{\pi}{2}.$$

We focus attention in the region of the skyrmion domain wall and develop an analysis valid to all orders in R^{-1} for skyrmions of large radius. The leading behavior of the solution as $R \rightarrow \infty$ is obtained by neglecting the terms of Eq. (5) with r in the denominator. The emerging equation

$$\Theta'' - \frac{1}{2} \sin(2\Theta) = 0 \quad (6)$$

characterizes the leading behavior of the domain wall of the skyrmion and has solution

$$\Theta_0 = 2 \arctan(e^{-T}), \quad (7)$$

where

$$T = r - R, \quad |T| \ll R. \quad (8)$$

Thus, the leading approximation of the skyrmion domain wall profile is independent of the radius when the radius is large. The constants of integration follow from the requirements $\Theta_0 = \frac{\pi}{2}$ when $T = 0$ and $\Theta_0 \rightarrow 0$ as $T \rightarrow \infty$. Past the domain wall, in the far field, the behavior is similar to the one of skyrmions of small radius [30].

We calculate easily the following quantities that will be used below,

$$\Theta'_0 = -\operatorname{sech} T, \quad \cos(2\Theta_0) = 1 - 2\operatorname{sech}^2 T, \quad \sin(2\Theta_0) = 2\operatorname{sech} T \tanh T, \quad \sin^2 \Theta_0 = \operatorname{sech}^2 T. \quad (9)$$

Proceeding to a higher order analysis, we use the radius R as the parameter of the problem. We construct an asymptotic series for the profile Θ in negative powers of R to all orders. The profile $\Theta(T)$ is expanded to an asymptotic series for large R ,

$$\Theta = \Theta_0 + \tilde{\Theta}, \quad \tilde{\Theta} = \frac{\Theta_1}{R} + \frac{\Theta_2}{R^2} + \frac{\Theta_3}{R^3} + \dots. \quad (10)$$

$\Theta_0(T)$ is given by Eq. (7) and $\Theta_1, \Theta_2, \Theta_3, \dots$ are also functions of T . Necessarily ϵ must be expressed in terms of the parameter R . We choose the same form of asymptotic expansion as for Θ ,

$$\epsilon = \epsilon_0 + \frac{\epsilon_1}{R} + \frac{\epsilon_2}{R^2} + \frac{\epsilon_3}{R^3} + \dots. \quad (11)$$

We introduce the expansion

$$\frac{1}{r} = \frac{\sigma}{R}, \quad \sigma = 1 - \frac{T}{R} + \frac{T^2}{R^2} + \dots \quad (12)$$

and we isolate the leading Taylor terms of the functions

$$\cos(2\tilde{\Theta}) = 1 + C(2\tilde{\Theta}), \quad \sin(2\tilde{\Theta}) = 2\tilde{\Theta} + S(2\tilde{\Theta}). \quad (13)$$

Inserting the series (10) for Θ into Eq. (5), applying the identities of trigonometric addition and using Eqs. (11), (12), (13) obtains

$$\tilde{\Theta}'' - \cos(2\Theta_0)\tilde{\Theta} = \tilde{g} \quad (14)$$

where the prime denotes differentiation with respect to T , and

$$\tilde{g} = \frac{g_1}{R} + \frac{g_2}{R^2} + \frac{g_3}{R^3} + \dots. \quad (15)$$

The explicit form of \tilde{g} is given in Eq. (A.1). The hierarchy of linear nonhomogeneous equations for the functions Θ_n is obtained directly from Eq. (14),

$$\Theta_n'' - (\cos 2\Theta_0)\Theta_n = g_n, \quad n = 1, 2, 3, \dots. \quad (16)$$

The forcing term g_n of the equation for Θ_n may depend only on the functions Θ_l with $l \leq n - 1$. All equations have the same homogeneous part. All equations satisfy the initial condition $\Theta_n(T = 0) = 0$. Indeed, according to the definition of the radius R , we have $\Theta(R) = \frac{\pi}{2}$; according to Eq. (7), we have $\Theta_0(T = 0) = \Theta_0(r = R) = \frac{\pi}{2}$. Necessarily, all the corrector functions Θ_n equal zero at $r = R$. We also require that Θ_n decays as $|T|$ increases. The requirement follows from the necessity that the corrector functions for large $|T|$ are matched with corresponding asymptotic contributions of the solution parts emanating from $r = 0$ and r at infinity over an intermediate spatial region (see Sec. 5).

The homogeneous equation corresponding to the hierarchy (16) is

$$\Theta_H'' - (1 - 2\operatorname{sech}^2 T)\Theta_H = 0. \quad (17)$$

This equation describes the motion of a quantum mechanical particle in a potential well (see, e.g., Ref. [32], page 73). The potential equaling negative $\text{sech}^2 T$ is one of the Bargmann reflectionless potentials, a class of potentials of the one-dimensional Schrödinger operator having bound states with negative energy and zero reflection coefficient for all positive energies [33]. Eq. (17) has the explicit basis solutions

$$H_1 = \text{sech } T, \quad H_2 = \sinh T + T \text{sech } T. \quad (18)$$

Their Wronskian is given by

$$\det \begin{pmatrix} H_1 & H_2 \\ H_1' & H_2' \end{pmatrix} = 2. \quad (19)$$

Using the formula of the variation of constants, we obtain

$$\Theta_n = -\frac{1}{2}H_1(T) \int_0^T g_n(\tau)H_2(\tau) d\tau + \frac{1}{2}H_2(T) \int_{-\infty}^T g_n(\tau)H_1(\tau) d\tau, \quad n = 1, 2, 3, \dots \quad (20)$$

The decay condition on Θ imposes the solvability condition

$$\int_{-\infty}^{\infty} g_n(\tau)H_1(\tau) d\tau = 0, \quad n = 1, 2, 3, \dots \quad (21)$$

The condition is obtained, by integrating over \mathbb{R} the Eq. (16) multiplied by $H_1 = \text{sech } T$, then integrating by parts twice and recalling that $H_1(T)$ is a solution of the homogeneous Eq. (17).

The calculation of the Θ_n is recursive; in order to demonstrate the calculational pattern, we examine the explicit form of the functions g_1, g_2, g_3

$$\begin{aligned} g_1 &= -(\Theta_0' + 2\epsilon_0 \sin^2 \Theta_0) \\ g_2 &= T(\Theta_0' + 2\epsilon_0 \sin^2 \Theta_0) - 2\epsilon_1 \sin^2 \Theta_0 + \sin 2\Theta_0 \left(\frac{1}{2} - 2\epsilon_0 \Theta_1 - \Theta_1^2 \right) - \Theta_1' \\ g_3 &= -T^2(\Theta_0' + 2\epsilon_0 \sin^2 \Theta_0) + 2(T\epsilon_1 - \epsilon_2) \sin^2 \Theta_0 + T\Theta_1' - \Theta_2' \\ &\quad + \sin 2\Theta_0 [-T + (T\epsilon_0 - \epsilon_1)2\Theta_1 - 2\epsilon_0\Theta_2 - 2\Theta_1\Theta_2] + \cos 2\Theta_0 \left(\Theta_1 - 2\epsilon_0\Theta_1^2 - \frac{2}{3}\Theta_1^3 \right). \end{aligned} \quad (22)$$

We make the following observations

1. Θ_0 is an odd function of T , thus, g_1 is even. Inserting g_1 into the solvability condition (21), produces the value of ϵ_0 .
2. The fact that g_1 in Eq. (20) is even implies that also Θ_1 is even.
3. All the terms of g_2 are odd with the exception of the term multiplied by ϵ_1 , which is even. Inserting g_2 into the solvability condition (21), produces $\epsilon_1 = 0$. Thus, g_2 is odd.
4. The fact that g_2 in Eq. (20) is odd implies that also Θ_2 is odd.
5. All terms of g_3 are even. Inserting g_3 into the solvability condition (21) produces the value of ϵ_2 .

The cycle continues periodically according to the flow chart

$$\underbrace{\Theta_0}_{\text{odd}} \rightarrow \underbrace{g_1}_{\text{even}} \rightarrow \underbrace{\begin{Bmatrix} \epsilon_0 \\ \Theta_1 \end{Bmatrix}}_{\text{even}} \rightarrow \underbrace{g_2}_{\text{odd}} \rightarrow \underbrace{\begin{Bmatrix} \epsilon_1 = 0 \\ \Theta_2 \end{Bmatrix}}_{\text{odd}} \rightarrow \underbrace{g_3}_{\text{even}} \rightarrow \underbrace{\begin{Bmatrix} \epsilon_2 \\ \Theta_3 \end{Bmatrix}}_{\text{even}} \rightarrow \underbrace{g_4}_{\text{odd}} \rightarrow \underbrace{\begin{Bmatrix} \epsilon_3 = 0 \\ \Theta_4 \end{Bmatrix}}_{\text{odd}} \rightarrow \dots$$

with odd indexed g_n and Θ_n being even and even indexed g_n and Θ_n being odd.

The parity results stated here are proved in the following theorem.

Theorem 1. *Let $\epsilon_{2i-1} = 0$ for $i = 1, 2, 3, \dots$. Then, the following parity conditions hold.*

1. For all $n \geq 1$, the functions $g_n = g_n(T)$ are even if n is odd and they are odd if n is even.
2. The same is true for the functions $\Theta_n = \Theta_n(T)$, for $n \geq 0$.

The proof of the theorem, involving some subtlety, is relegated to Appendix A in order to allow the flow of the calculation to be continued uninterrupted.

The coefficient ϵ_n makes its first appearance in the expression of g_{n+1} multiplying the term $-2 \operatorname{sech}^2 T$ for every n . Using this, the solvability condition (21) produces the values

$$\epsilon_n = \frac{1}{\pi} \int_{-\infty}^{\infty} (\operatorname{sech} \tau) g_{n+1}(\tau)|_{\epsilon_n=0} d\tau, \quad n = 0, 1, 2, 3, \dots \quad (23)$$

For every odd n the integrand is odd giving $\epsilon_n = 0$, i.e., all odd indexed ϵ_n vanish. As a result, relation (11) of the dimensionless DM parameter with the skyrmion radius is simplified to

$$\epsilon = \epsilon_0 + \frac{\epsilon_2}{R^2} + \frac{\epsilon_4}{R^4} + \frac{\epsilon_6}{R^6} + \dots \quad (24)$$

3.1. A virial identity and the values of ϵ_0 and ϵ_2

We multiply Eq. (5) by $2r\Theta'$ and we integrate over the r axis. After straightforward algebraic and trigonometric manipulations, we obtain

$$\int_0^{\infty} \left[(r\Theta'^2)' + \Theta'^2 - \left(r + \frac{1}{r} \right) (\sin^2 \Theta)' + 4\epsilon (\sin^2 \Theta)\Theta' \right] dr = 0. \quad (25)$$

The first and last terms under the integral are exact derivatives; they integrate to zero and to $-2\pi\epsilon$ respectively. Performing an integration by parts, we obtain the virial identity that is satisfied by all skyrmions and is crucial for our calculation,

$$\int_0^{\infty} \left[\Theta'^2 + \left(1 - \frac{1}{r^2} \right) \sin^2 \Theta \right] dr = 2\pi\epsilon. \quad (26)$$

The following theorem, based on relation (26), provides an explicit formulae for ϵ_0 and ϵ_2 .

Theorem 2. *The DM parameter ϵ satisfies the relation*

$$\epsilon = \frac{2}{\pi} - \frac{1}{\pi R^2} \left(1 + \frac{1}{2} \int_{-\infty}^{\infty} \Theta_1 g_1 dT \right) + O(R^{-4}). \quad (27)$$

Proof. We take the limit $R \rightarrow \infty$ in the integral law (26). The integral of $\sin^2 \Theta/r^2$ converges to zero; the integrand decays exponentially in the core and far field of the skyrmion. In the limit, we are left with

$$\int_{-\infty}^{\infty} (\Theta_0'^2 + \sin^2 \Theta_0) dT = 2\pi\epsilon_0. \quad (28)$$

The integral in Eq. (28) is calculated using Eqs. (9) and equals 4. The critical value

$$\epsilon_0 = \frac{2}{\pi} \quad (29)$$

follows directly.

For the determination of ϵ_2 we expand the virial identity (26) in powers up to $O(R^{-2})$. We insert $\Theta = \Theta_0 + \tilde{\Theta}$, and make T the integration variable. The manipulation, which involves integrations by parts resulting in significant cancellations, is relegated to Appendix B.1. We obtain

$$\epsilon_2 = -\frac{1}{\pi} \left(1 + \frac{1}{2} \int_{-\infty}^{\infty} \Theta_1 g_1 dT \right). \quad (30)$$

The value of the latter integral is found in Appendix B.3. Inserting the value given in Eq. (B.16) into Eq. (30) we find

$$\epsilon_2 = -\frac{0.9605}{\pi} \approx -0.3057 \quad (31)$$

It agrees with the result in Eq. (60) found by a different method in Sec. 6. \square

In Ref. [34], the value $\epsilon_2 = -1/\pi$ was found by an energy minimization argument that takes only Θ_0 into account.

4. The skyrmion core and the skyrmion far field

On the core where Θ is close to π , and on the far field where Θ is close to 0, Eq. (5) reduces by linearization to the modified Bessel equation

$$r^2\theta'' + r\theta' - (r^2 + 1)\theta = 0, \quad (32)$$

where $\theta = \Theta$ in the far field with $\theta \rightarrow 0$ as $r \rightarrow \infty$ and $\theta = \pi - \Theta$ in the core, with $\theta(0) = 0$. The equation is solved exactly, in terms of the modified Bessel functions $I_1(r)$ and $K_1(r)$. Enforcing the boundary conditions, we obtain

$$\Theta = \begin{cases} \pi - C_1 I_1(r), & \text{(core)} \\ C_2 K_1(r) & \text{(far field)}, \end{cases} \quad (33)$$

where C_1 and C_2 are constants. The modified Bessel function K_1 has been used in a similar context to describe the far field of dynamic solitons in Ref. [35].

Inserting the power series expansion of I_1 , from formula 9.6.10 of Ref. [36] obtains

$$\Theta = \pi - \frac{1}{2}C_1 r \sum_{n=0}^{\infty} \frac{\left(\frac{1}{4}r^2\right)^n}{n!(n+1)!}. \quad (34)$$

Using the asymptotic expansions of I_1 and K_1 for large values of r , from formulae 9.7.1 and 9.7.2 of Ref. [36], where the coefficients a_n are defined ($a_0 = 1$), obtains

$$\Theta \sim \pi - \frac{C_1 e^r}{\sqrt{2\pi r}} \sum_{n=0}^{\infty} \frac{(-1)^n a_n}{r^n} \quad \text{(core);} \quad \Theta \sim C_2 \sqrt{\frac{\pi}{2r}} e^{-r} \sum_{n=0}^{\infty} \frac{a_n}{r^n} \quad \text{(far field)}. \quad (35)$$

In order to match these equations in the region $1 \ll |T| \ll R$, with the profile equation of the domain wall, we insert the substitution

$$r = R \left(1 + \frac{T}{R}\right), \quad (36)$$

into Eqs. (35). Utilizing the binomial expansion with exponents $-(n + \frac{1}{2})$ and recalling that $T < 0$ in the core, $T > 0$ in the far field, we obtain

$$\begin{aligned} \Theta &\sim \pi + \frac{C_1 e^R e^{-|T|}}{\sqrt{2\pi R}} \sum_{n=0}^{\infty} \frac{(-1)^{n-1} Q_n(T)}{R^n} \quad \text{(core)} \\ \Theta &\sim C_2 \sqrt{\frac{\pi}{2R}} e^{-R} e^{-|T|} \sum_{n=0}^{\infty} \frac{Q_n(T)}{R^n} \quad \text{(far field)} \end{aligned} \quad 1 \ll T \ll R \quad (37)$$

where

$$Q_n(T) = \sum_{k=0}^n a_{n-k} \binom{-n+k-\frac{1}{2}}{k} |T|^k, \quad n = 0, 1, 2, 3 \dots \quad (38)$$

5. Asymptotic matching

We now match the expressions of the azimuthal angle Θ of the domain wall to the ones of the skyrmion core and of the far field. The two transition regions are characterized by the asymptotic relation $1 \ll |T| \ll R$, with $T < 0$ in the core/domain wall region and $T > 0$ in the far-field/domain wall region; in each of the two regions, we require that the asymptotic expressions of Θ , from either side of the transition, be identical to each other. In order to achieve this, we first need to calculate the large $|T|$ behavior of the domain wall expression for Θ . The azimuthal angle Θ in the domain wall is given by

$$\Theta = \sum_{n=0}^{\infty} \frac{\Theta_n(T)}{R^n}, \quad \Theta_0 = 2 \arctan e^{-T}, \quad (39)$$

derived above.

5.1. Leading order match

In the limit $|T| \rightarrow \infty$, Eq. (39) reduces to

$$\Theta_0(T) = \begin{cases} \pi - 2e^{-|T|} + O(e^{-3|T|}), & T < 0 \\ 2e^{-|T|} + O(e^{-3|T|}), & T > 0, \end{cases} \quad (40)$$

Identifying this with the leading order contribution ($n = 0$) of Eq. (37), obtains the values of the constants

$$C_1 = e^{-R} \sqrt{8\pi R}, \quad C_2 = e^R \sqrt{\frac{8R}{\pi}}. \quad (41)$$

Inserting the values of C_1 and C_2 from Eq. (41) into Eq. (37), we obtain, in $1 \ll T \ll R$,

$$\Theta \sim \pi + 2e^{-|T|} \sum_{n=0}^{\infty} \frac{(-1)^{n-1} Q_n(T)}{R^n} \quad (\text{core}); \quad \Theta \sim 2e^{-|T|} \sum_{n=0}^{\infty} \frac{Q_n(T)}{R^n} \quad (\text{far field}) \quad (42)$$

where Q_n are given in Eq. (38).

The skyrmion profile is linear to leading order with an exponentially small slope, close to the skyrmion center,

$$\Theta \approx \pi - e^{-R} \sqrt{2\pi R} r, \quad r \ll 1. \quad (43)$$

With r increasing, the deviation of the profile from the value π attains exponential growth, which is held in check throughout the skyrmion core by the small exponential factor e^{-R} . Substituting the value of C_1 from Eq. (41) in Eq. (35) we obtain, in the core,

$$\Theta \approx \pi - 2 \sqrt{\frac{R}{r}} e^{r-R}, \quad 1 \ll r < R, \quad 1 \ll R - r. \quad (44)$$

The leading approximation of the skyrmion domain wall profile is independent of the radius when the radius is large, (see Sec. 3). Past the domain wall, in the far field, the behavior is similar to the one of skyrmions of small radius [30]. We have

$$\Theta \approx 2 \sqrt{\frac{R}{r}} e^{-(r-R)}, \quad r > R, \quad r - R \gg 1, \quad (45)$$

following from Eq. (35) (far field) and the value of the constant C_2 from Eq. (41).

5.2. Matching to all orders: Large $|T|$ asymptotics

Theorem 3. In the limit $|T| \rightarrow \infty$, we have

$$\Theta_0(T) = \begin{cases} \pi - 2e^{-|T|} + O(e^{-3|T|}), & T < 0 \\ 2e^{-|T|} + O(e^{-3|T|}), & T > 0, \end{cases} \quad (46)$$

$$\begin{aligned} g_n(T) &= [G_n(T)e^{-|T|} + O(e^{-2|T|})](\text{sign } T)^{n-1}, \\ \Theta_n(T) &= 2 [P_n(T)e^{-|T|} + O(e^{-2|T|})](\text{sign } T)^{n-1} \end{aligned} \quad n = 1, 2, 3 \dots \quad (47)$$

where $G_n(T)$ and $P_n(T)$ are polynomials of $|T|$ with $G_n(T)$ having degree $n - 1$ and $P_n(T)$ degree n .

Eq. (46) repeats Eq. (40) so that the theorem makes a complete statement.

Proof. We begin our large $|T|$ analysis with the observation that the quantity \tilde{g} of Eq. (A.1) is enormously simplified in the regime of large $|T|$. Recalling that the functions $\sin \Theta_0, \Theta_1, \Theta_2, \Theta_3, \dots$ contain the factor $e^{-|T|}$, any products of these can be neglected. Thus, only terms of \tilde{g} that are linear in these functions remain in play. We obtain

$$\tilde{g} = -\frac{\sigma}{R}\Theta'_0 + \frac{\sigma^2}{2R^2}\sin(2\Theta_0) - \frac{\sigma}{R}\tilde{\Theta}' + \frac{\sigma^2}{R^2}\cos(2\Theta_0)\tilde{\Theta} + O(e^{-2|T|}). \quad (48)$$

Inserting Eqs. (9) considered in the large $|T|$ limit,

$$\Theta'_0 = -2e^{-|T|} + O(e^{-2|T|}), \quad \sin 2\Theta_0 = 2e^{-|T|}\text{sign}T + O(e^{-2|T|}), \quad \cos 2\Theta_0 = 1 + (e^{-2|T|}), \quad (49)$$

obtains

$$\tilde{g} = e^{-|T|} \left[\frac{\sigma}{R}(2 - \tilde{\Theta}') + \frac{\sigma^2}{R^2}(\text{sign}T + \tilde{\Theta}) \right] + O(e^{-2|T|}) \quad (50)$$

One calculates easily

$$g_1 = 2e^{-|T|} + O(e^{-2|T|}). \quad (51)$$

In the large $|T|$ limit, Eq. (16) for $n = 1$ becomes

$$\Theta'_1 - \Theta_1 = 2e^{-|T|} + O(e^{-2|T|}). \quad (52)$$

with decaying solution

$$\begin{aligned} \Theta_1 &= (-|T| + c_1)e^{-|T|} + O(e^{-2|T|}), & |T| \gg 1, \\ \Theta'_1 &= (|T| - c_1 - 1)e^{-|T|}\text{sign}T + O(e^{-2|T|}), & |T| \gg 1 \end{aligned} \quad (53)$$

where c_1 is a free variable (see Sec. 5). The zero condition on Θ_1 at $T = 0$ cannot be used here; the present solution holds only in the region where $|T|$ is large. We can now calculate g_2 , using Eq. (50). We obtain

$$g_2 = [(|T| + c_1 + 2)e^{-|T|} + O(e^{-2|T|})]\text{sign } T, \quad |T| \gg 1. \quad (54)$$

Eq. (16) for $n = 2$ becomes

$$\Theta''_2 - \Theta_2 = [(|T| + c_1 + 2)e^{-|T|} + O(e^{-2|T|})]\text{sign } T, \quad |T| \gg 1 \quad (55)$$

and its solution has the form

$$\Theta_2 = [(a|T|^2 + b|T| + c_2)e^{-|T|} + O(e^{-2|T|})]\text{sign}T, \quad |T| \gg 1. \quad (56)$$

The constants a and b are calculated from the requirement that Θ_2 satisfies Eq. (55). The constant c_2 is a free variable (see Sec. 5). The procedure continues, clearly, in the same pattern as the index n increases. The arising odd/even parity pattern of the functions Θ_n is exactly as asserted by theorem 1. This completes the proof of the theorem. \square

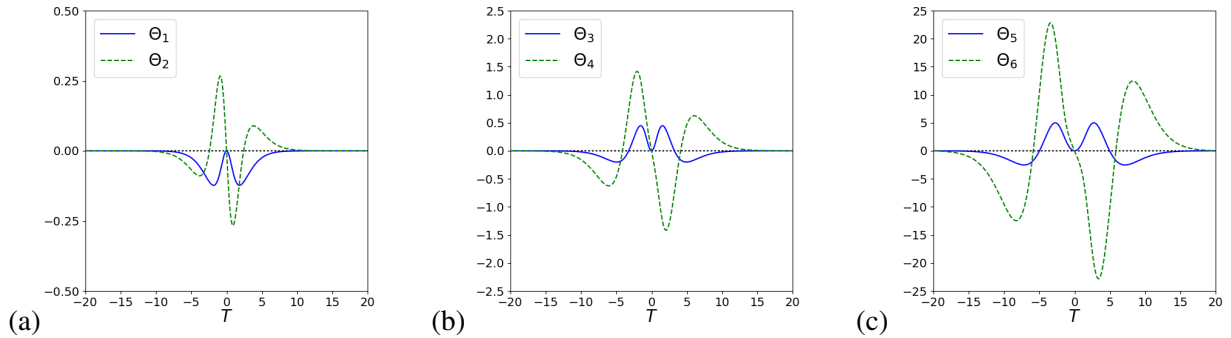


Figure 2: The functions (a) Θ_1 , Θ_2 , (b) Θ_3 , Θ_4 , and (c) Θ_5 , Θ_6 calculated by numerical evaluation of the integrals in Eq. (20). As seen by the change of scale of the vertical axis in the three entries, the values of the functions Θ_n increase fast with increasing index n . Note the even parity of the odd indexed functions and the odd parity of the even indexed ones with respect to the variable $T = r - R$.

5.3. Matching to all orders: Matching conditions

Comparing Eqs. (42) with Eqs. (39) and (47), we obtain the matching conditions

$$P_n(T) = Q_n(T), \quad n = 1, 2, 3, \dots, \quad (57)$$

that identify the two sets of polynomials and match the domain wall series for the azimuthal function Θ with the two core/far field series on the overlap regions. This matching provides the values of the free variables c_1, c_2, \dots in Eqs. (53), (56), etc. We have, thus, a unified asymptotic solution of Eq. (5) that satisfies the boundary condition $\Theta = \pi$ at $r = 0$ and decays at infinity.

6. Numerics

We proceed to find $\Theta_1, \Theta_2, \Theta_3, \Theta_4, \Theta_5, \Theta_6$ by applying Eq. (20). The expressions for g_n for higher n are long and they have been derived using the mathematics software system SageMath [37]. The derivatives Θ'_n needed in the expressions of g_n are found by finite differences in the numerical calculation. Fig. 2 shows functions Θ_1 through Θ_6 . As expected from Theorem 1, odd indexed Θ_n 's are even functions of T and even indexed ones are odd. Functions Θ_n with higher index n take higher values and they take significant values over larger intervals of T . These features have consequences for the quality of the approximation, especially for small R , as we shall see in the following.

We have calculated by a shooting method the skyrmion profiles, which are solutions of Eq. (5), for various values of the parameter ϵ . (We have actually solved an equation for the stereographic projection of the magnetization vector which is equivalent to Eq. (5), as described in Ref. [30].) They are shown in Fig. 3 by small circles for two values of the parameter ϵ . In Fig. 3a, we have $\epsilon = 0.60$ that gives a skyrmion of radius $R = 3.29 \ell_w$. The profile at the skyrmion core is approximated very well by the solution given in Eq. (33) with the coefficient given in Eq. (41), and is shown as an orange dashed line in the figure. The blue solid line shows the one-dimensional domain wall profile Θ_0 , shown in Eq. (7), centred at the skyrmion radius position $r = R$. The red line shows the series solution (10) for Θ up to the term $O(1/R^6)$. The approximation of the skyrmion profile is excellent for all r except near the skyrmion center $r = 0$. In Fig. 3b, we have $\epsilon = 0.55$ and a smaller skyrmion radius $R = 2.02 \ell_w$. The solution (33) still gives an excellent approximation at the skyrmion core. The green line shows the series solution (10) for Θ up to the term $O(1/R^2)$ and obtains a good approximation of the profile, especially around the skyrmion radius

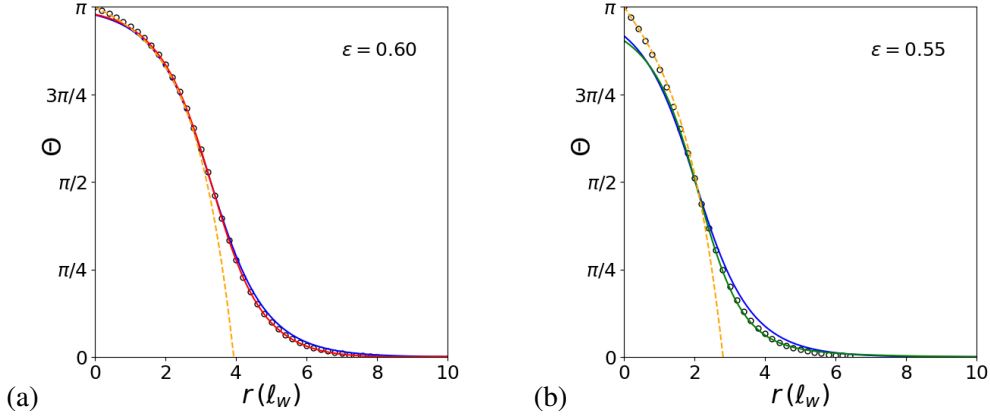


Figure 3: The profile of a skyrmion $\Theta(r)$ is shown by small circles for two values of the parameter ϵ , obtained numerically by solving the original Eq. (5) using a shooting method. The blue line shows Θ_0 , which is the one-dimensional domain wall profile. The orange line shows the solution (33) for the skyrmion profile at the core, obtained by linearizing the original equation about $\Theta = \pi$. (a) For $\epsilon = 0.60$ the skyrmion has a radius $R = 3.29 \ell_w$, as obtained by the shooting method. The red line shows the series (10) summed up to the term Θ_6 . (b) For $\epsilon = 0.55$ the skyrmion has a radius $R = 2.02 \ell_w$. For this smaller value of R the optimal point of truncation of the series occurs at the term Θ_2 . The green line shows the series (10) summed up to and including the term Θ_2 .

and for $r > R$. At the value $\epsilon = 0.55$ of Fig. 3b, this is the optimal truncation of the series. Indeed, including terms of order higher than $O(1/R^2)$, requires that they, too, satisfy the asymptotic requirement that the contribution at each order be significantly smaller than the one at the order that precedes it. This results into the narrowing of the range of the asymptotic parameter ϵ , that leaves the value $\epsilon = 0.55$ outside it. The narrowing of the range of ϵ is consistent with the fact, shown in Fig. 2, that an increasing index n produces Θ_n 's with rapidly increasing values.

We now calculate the numerical values of ϵ_n from Eq. (23). We obtain

$$\epsilon \approx \frac{2}{\pi} - \frac{0.3057}{R^2} - \frac{0.8792}{R^4} - \frac{5.901}{R^6}, \quad R \gg 1, \quad (58)$$

where

$$\epsilon_0 = \frac{1}{\pi} \int_{-\infty}^{\infty} \text{sech}^2 \tau \, d\tau = \frac{2}{\pi} \quad (59)$$

is obtained analytically while

$$\epsilon_2 \approx -0.3057, \quad \epsilon_4 \approx -0.8792, \quad \epsilon_6 \approx -5.901 \quad (60)$$

are found by numerical integration. The values of ϵ_0, ϵ_2 agree perfectly with the values found in Sec. 3.1 by a different method. Inverting Eq. (24) we obtain the skyrmion radius versus the parameter ϵ ,

$$R = \frac{|\epsilon_2|^{1/2}}{\tilde{\epsilon}^{1/2}} + O(\tilde{\epsilon}^{1/2}), \quad \tilde{\epsilon} = \frac{2}{\pi} - \epsilon. \quad (61)$$

Fig. 4 shows by open circles the skyrmion radius extracted from the calculation of the skyrmion profiles by the shooting method. These data are compared with formula (58) for the successive approximations up to and including order $O(1/R^2)$, $O(1/R^4)$, and $O(1/R^6)$. The approximation is excellent for large R and it

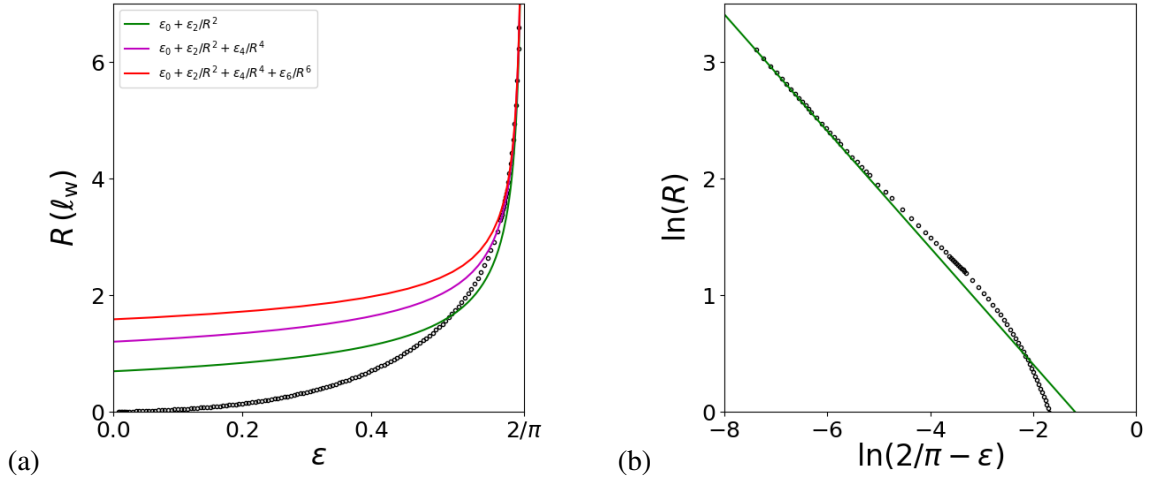


Figure 4: (a) The skyrmion radius R found numerically by solving the original equation (5) for various values of ϵ is shown by open circles. Relation (58) is shown by the colored lines to order $O(1/R^2)$, $O(1/R^4)$, $O(1/R^6)$ as indicated in the legend. The curves diverge at the critical value $\epsilon = 2/\pi$. The successive approximations enhance the accuracy as R increases. The logarithm of R as a function of the logarithm of the difference of ϵ from the critical value $\epsilon_0 = 2/\pi$. The green lines show relation (58) to order $O(1/R^2)$, i.e., $\ln(R) = \frac{1}{2}[\ln|\epsilon_2| - \ln(\epsilon_0 - \epsilon)]$. The open dots show numerical results and they approach the theoretical green line as $R \rightarrow \infty$ and $\epsilon \rightarrow \epsilon_0$.

is improving as we add higher order terms, as seen in the blow-up in Fig. 4b. For smaller R , higher order approximations give larger deviations from the correct result, especially when the term $O(1/R^6)$ is included. This is a consequence of the increasing error in the asymptotic series for small values of R as was discussed in relation to Fig. 3.

7. Energy of skyrmion

Let us denote by $E_{\text{ex}}, E_{\text{an}}, E_{\text{DM}}$ the exchange, anisotropy and DM energy terms in the total energy (4). Using a standard scaling argument [38] one proves that any localized configuration that is a minimum of the energy in an infinitely extended two-dimensional system, such as a skyrmion, satisfies

$$2E_{\text{an}} + E_{\text{DM}} = 0. \quad (62)$$

In a one dimensional system the same argument gives for minima of the energy, such as a domain wall,

$$E_{\text{ex}} - E_{\text{an}} = 0. \quad (63)$$

In the limit $\epsilon \rightarrow 2/\pi$, the latter relation is correct to leading order also for a skyrmion, as the leading approximation for the skyrmion profile, in this limit, is Θ_0 . Thus, in the limit, a skyrmion satisfies both (62) and (63), and these are combined to give

$$E_{\text{ex}} = E_{\text{an}} = -\frac{E_{\text{DM}}}{2} \quad \text{when} \quad \epsilon \rightarrow \frac{2}{\pi}. \quad (64)$$

The total skyrmion energy is

$$E = E_{\text{ex}} + E_{\text{an}} + E_{\text{DM}} = 0 \quad \text{when} \quad \epsilon \rightarrow \frac{2}{\pi}. \quad (65)$$

We give a full asymptotic series for the energy in the following theorem.

Theorem 4. *All three forms of skyrmion energy in Eq. (4), exchange, anisotropy and DM, have asymptotic expansions in which only odd powers of R are present,*

$$E_{\text{ex}} = 2\pi R + \frac{E_{\text{ex},1}}{R} + \frac{E_{\text{ex},3}}{R^3} + \dots, \quad E_{\text{an}} = 2\pi R + \frac{E_{\text{an},1}}{R} + \frac{E_{\text{an},3}}{R^3} + \dots, \quad E_{\text{DM}} = -4\pi R + \frac{E_{\text{DM},1}}{R} + \frac{E_{\text{DM},3}}{R^3} + \dots, \quad (66)$$

The three leading terms sum up to zero; the total energy is

$$E \sim \frac{E_1}{R} + \frac{E_3}{R^3} + \frac{E_5}{R^5} + \dots, \quad E_1 = 4\pi^2 |\epsilon_2|, \quad R \rightarrow \infty. \quad (67)$$

The skyrmion energy tends to zero, as ϵ increases, approaching its critical value, with a rate of convergence

$$E \sim (4\pi^2 |\epsilon_2|^{1/2}) \tilde{\epsilon}^{1/2} + O(\tilde{\epsilon}^{3/2}), \quad \tilde{\epsilon} = \frac{2}{\pi} - \epsilon. \quad (68)$$

Proof. We classify the functions of the form $f(T)R^n$, where the function f can be odd or even and the power n can be any integer, according to the following table.

Class	n	f
A	odd	even
B	even	odd
C	odd	odd
D	even	even

It suffices to prove that every term of the expression under the energy integral (4) belongs to class $A + B + C$, meaning that it is a sum of terms from the classes A, B and C. The integration will eliminate the terms in B and C; only odd powers of R will participate in the expression of each of the three components of the energy and, hence, in the total energy.

In order to simplify the notation, we use the symbol of the class to also denote the class elements as well as sums of the class elements. Thus,

$$\Theta_0 + \frac{\Theta_2}{R^2} + \frac{\Theta_4}{R^4} + \dots \equiv B, \quad \frac{\Theta_1}{R} + \frac{\Theta_3}{R^3} + \frac{\Theta_5}{R^5} + \dots \equiv A, \quad T \equiv B, \quad R \equiv A. \quad (69)$$

We notice that

$$A^2 \equiv B^2 \equiv C^2 \equiv D^2 \equiv D, \quad AB \equiv C, \quad AC \equiv B, \quad BC \equiv A, \quad AD \equiv A, \quad BD \equiv B, \quad A' \equiv C, \quad B' \equiv D. \quad (70)$$

We also have

$$\sin A \equiv A, \quad \sin B \equiv B, \quad \cos A \equiv \cos B \equiv D. \quad (71)$$

By applying trigonometric identities, we obtain

$$\sin(A + B) \equiv AD + BD \equiv A + B, \quad \cos(A + B) \equiv DD + AB \equiv D + C. \quad (72)$$

We perform the calculation term by term, expressing $\sin^2 \Theta$ as $\frac{1}{2}(1 - \cos 2\Theta)$.

1. Term $r \left(\frac{d\Theta}{dr} \right)^2 \equiv (R + T)(A + B)^2 \equiv (A + B)(C^2 + CD + D^2) \equiv (A + B)(D + C) \equiv A + B$.
2. Term $r \frac{d\Theta}{dr} \equiv (A + B)(C + D) \equiv A + B$.

3. Term $\sin 2\Theta \equiv \sin(A + B) \equiv \sin(A + B) \equiv A + B$.
4. Term $r + \frac{1}{r} \equiv A + B$ (see Eq. (12)).
5. Term $\left(r + \frac{1}{r}\right) \cos 2\Theta \equiv (A + B)(D + C) \equiv A + B$.

This shows that only odd powers of R are present.

The highest order term in the energy is $O(R)$ with the contributions of the three energy terms (exchange, anisotropy and DM) given by the corresponding three terms in the integral

$$2\pi R \int_{-\infty}^{\infty} \left\{ \frac{1}{2} \left(\frac{d\Theta_0}{dT} \right)^2 + \frac{1}{2} \sin^2 \Theta_0 + \frac{2}{\pi} \left(\frac{d\Theta_0}{dT} \right) \right\} dT. \quad (73)$$

Inserting the relevant quantities from Eqs. (9), we obtain the $O(R)$ terms in Eq. (66) for the individual energies. The $O(R)$ term in the total energy vanishes. The term $O(R^{-1})$ is calculated in Appendix B.2, giving the result of Eq. (67). Inserting Eq. (61) into Eq. (67), we obtain Eq. (68). \square

8. Conclusions

We have derived the profile of an axially symmetric skyrmion which is a solution of the time-independent Landau-Lifshitz equation in the case of large skyrmion radius R . The analysis is based on the asymptotic series (10) for Θ over the skyrmion domain wall and a key observation is the parity property detailed in Appendix A. That is, the functions $\Theta_n(T)$ in the series are odd functions of T if n is even and they are even functions, if n is odd. The series formulae at the core and the far field, derived in Sec. 4, are matched to the domain wall to all orders in inverse powers of R , as shown in Sec. 5. As a result, the skyrmion profile is represented over the full spatial extent.

A breakdown of skyrmion solutions, via a diverging radius, occurs when approaching the threshold value $\epsilon = 2/\pi$ from below. This coincides with the value at which the transition from the ferromagnetic regime to the helical regime takes place.

The parity properties of the asymptotic expansion of Θ have many consequences. The DM parameter ϵ is expressed as an even asymptotic series in inverse powers of R . The skyrmion energy E is expressed as an odd asymptotic series in inverse powers of R . In addition, the energy goes to zero as the skyrmion radius goes to infinity.

We expect that the analytical formulae for the skyrmion profile will provide a powerful tool in order to analyse recent detailed experimental observations of skyrmions and study quantitatively dynamical phenomena involving individual skyrmions. The details of the skyrmion profile could prove essential for the manipulation of individual skyrmions. The present analytical results can also guide numerical studies for skyrmions in complex systems such as in ferromagnetically or antiferromagnetically coupled multilayers [39].

The skyrmion found within the time-independent Landau-Lifshitz equation for the magnetization in ferromagnets is identical to the static skyrmion in antiferromagnets described via the Néel vector within a time-independent σ -model. Therefore, all results in this paper apply also to antiferromagnetic skyrmions. Traveling skyrmion solutions in antiferromagnets have been found as traveling wave solutions within a σ -model [40]. As these are not axially symmetric, a generalization of the methods of this paper to non-static skyrmions is not straightforward. This remark applies to skyrmions in both antiferromagnets and ferromagnets.

A skyrmion can be stabilized by using an external field h , instead of the anisotropy term that was used in the present work. In that case, the ferromagnetic is the ground state for a field stronger than a critical

value, $h \geq h_c$, and the skyrmion is an excited state in this regime. For $h < h_c$, a skyrmion lattice is obtained. The energy of an individual skyrmion is zero at $h = h_c$ but its radius goes neither to zero nor does it diverge. Therefore, the limit of large skyrmion radius does not appear to be relevant for the case of skyrmions stabilized by an external field.

Acknowledgement

We are grateful to Stefan Blügel and to Alex Bogdanov for fruitful discussions. CM gratefully acknowledges financial support by the DFG under the grant no. ME 2273/3-1, and SK a Mercator fellowship as part of the previous grant. SV gratefully acknowledges financial support by the NSF through contract DMS-1211638. SK acknowledges funding from the Hellenic Foundation for Research and Innovation (HFRI) and the General Secretariat for Research and Technology (GSRT), under grant agreement No 871.

Appendix A. Parity theorem

Proceeding to the calculation at higher orders of $1/R$ we determine the formula for \tilde{g} utilizing Eqs. (12), (13). We obtain

$$\begin{aligned} \tilde{g} = & -\sigma \frac{\Theta'_0}{R} - \sigma \epsilon \frac{1 - \cos(2\Theta_0)}{R} + \sigma^2 \frac{\sin(2\Theta_0)}{2R^2} - \sigma \frac{\tilde{\Theta}'}{R} + \left(-\sigma \epsilon \frac{\sin(2\Theta_0)}{R} + \sigma^2 \frac{\cos(2\Theta_0)}{2R^2} \right) 2\tilde{\Theta} \\ & + \left(\frac{1}{2} \sin(2\Theta_0) + \sigma \epsilon \frac{\cos(2\Theta_0)}{R} + \sigma^2 \frac{\sin(2\Theta_0)}{2R^2} \right) C(2\tilde{\Theta}) + \left(\frac{1}{2} \cos(2\Theta_0) - \sigma \epsilon \frac{\sin(2\Theta_0)}{R} + \sigma^2 \frac{\cos(2\Theta_0)}{2R^2} \right) S(2\tilde{\Theta}). \end{aligned} \quad (\text{A.1})$$

The following theorem is instrumental for all calculations based on Eq. (16), and in particular for those presented in Sec. 3. The hypotheses of the theorem turn out to be necessary conditions for the existence of bounded solutions Θ_n .

Theorem. *Let $\epsilon_{2i-1} = 0$ for $i = 1, 2, 3, \dots$. Then, the following parity conditions hold.*

1. *For all $n \geq 1$, the functions $g_n = g_n(T)$ are even if n is odd and they are odd if n is even.*
2. *The same is true for the functions $\Theta_n = \Theta_n(T)$.*

Proof. It follows from Eq. (20) that g_n and Θ_n have the same parity. Therefore, it suffices to prove the theorem for the g_n . We already know that the theorem is true for $n = 1$. Clearly, only terms Θ_j with $j < n$ appear in the expression for g_n , so we can truncate $\tilde{\Theta}$ accordingly. We make the inductive assumption that the functions $g_1, g_2, g_3, \dots, g_{n-1}$ alternate in parity, with g_1 being even. We prove then that g_n follows the alternating parity pattern. We do this for each term of Eq. (A.1), working with

$$\delta = R^{-1}.$$

in order to avoid denominators. The alternating parity condition is, clearly, true for the first term of Eq. (A.1) namely, $\sigma \Theta'_0 \delta$. The alternating parity comes from the fact that σ is a power series in (δT) with nonzero coefficients; and the lowest degree contribution to the term is $\Theta'_0 \delta$, an even function of T . The parity condition is satisfied, in a similar way, for the following two terms of the equation, in which no Θ_j appears.

The verification for the terms in which only one Θ_j appears is equally straightforward. For example, the term before the first parenthesis, is the sum of terms $T^{m-1} \Theta'_{n-m} \delta^n$. The parity requirement is clearly satisfied

for $m = 1$, since taking the derivative changes the parity. Increasing the value of m by k introduces the factor T^k and also shifts the index of Θ backwards by k positions. According to our inductive assumption, the parity of the term is preserved.

More work is required to show that the parity condition holds for the terms that have the factor $C(\tilde{\Theta})$ or $S(\tilde{\Theta})$. According to the inductive assumption, the truncated

$$\tilde{\Theta} = \delta\Theta_1 + \delta^2\Theta_2 + \delta^3\Theta_3 + \dots + \delta^{n-1}\Theta_{n-1} \quad (\text{A.2})$$

has even functions of T multiplying the odd powers of δ and odd functions of T multiplying the even powers of δ . The general term of the expansions of $C(\tilde{\Theta})$ and $S(\tilde{\Theta})$ is represented by

$$\tilde{\Theta}^{\mathbf{k}} = (2\delta)^{\mathbf{k}\cdot\mathbf{q}}\Theta_1^{k_1}\Theta_2^{k_2}\dots\Theta_{n-1}^{k_{n-1}}, \quad (\text{A.3})$$

where $\mathbf{k} = (k_1, k_2, k_3, \dots, k_{n-1})$ with $k_i \in \{0, 1, 2, 3, \dots\}$, and where $\mathbf{q} = (1, 2, 3, \dots, n-1)$. The term $\tilde{\Theta}^{\mathbf{k}}$ is either even or odd, since the factors Θ_j are even or odd.

Claim.

- (a) All the terms in the expansion of $C(\tilde{\Theta})$ are even at even powers of δ and odd at odd powers of δ .
- (b) All the terms in the expansion of $S(\tilde{\Theta})$ are odd at even powers of δ and even at odd powers of δ .

In order to prove the claim, we utilize the notion of the parity of a number or a function. The parity equals zero in the case of evenness and it equals unity in the case of oddness of the number or function. We calculate the following three parities.

- (i) The parity of the exponent n in the order δ^n of a term $\tilde{\Theta}^{\mathbf{k}}$.
- (ii) The parity of the product $\Theta_1^{k_1}\Theta_2^{k_2}\dots\Theta_{n-1}^{k_{n-1}}$ in $\tilde{\Theta}^{\mathbf{k}}$.
- (iii) The parity of the number of the factors Θ_j in $\tilde{\Theta}^{\mathbf{k}}$, counting multiplicities.

We obtain the following.

- (i) The exponent of δ equals $n = \mathbf{k} \cdot \mathbf{q}$. For the calculation of the parity of n , we set $k_j q_j = 0$ if q_j is even (eliminates all the odd factors Θ_j) or if k_j is even (eliminates all factors Θ_j with even multiplicity). We are thus, keeping only the even factors with odd multiplicity. The parity is thus

$$N_{even} \equiv \# \text{ of factors } \Theta_j \text{ that are even functions with odd multiplicity mod}(2). \quad (\text{A.4})$$

- (ii) The second parity, which we denote by N_{odd} , equals

$$N_{odd} \equiv \# \text{ of odd factors with odd multiplicity mod}(2). \quad (\text{A.5})$$

- (iii) The parity of the number of the factors Θ_j in $\tilde{\Theta}^{\mathbf{k}}$, counting multiplicities is given by the sum $k_1 + k_2 + \dots + k_{n-1}$. It is an even number for the terms of $C(\tilde{\Theta})$ and an odd number for the terms of $S(\tilde{\Theta})$. The third parity, which we denote by N_{total} , equals

$$N_{total} \equiv \# \text{ of all factors of odd multiplicity mod}(2). \quad (\text{A.6})$$

Clearly, $N_{even} + N_{odd} \equiv N_{total} \pmod{2}$. Hence, $N_{total} \equiv 0$ in the case of $C(\tilde{\Theta})$ and $N_{total} \equiv 1$ for $S(\tilde{\Theta})$. Parities 1 and 2 agree with each other in the terms of $C(\tilde{\Theta})$ and differ from each other in the terms of $S(\tilde{\Theta})$. This proves the claim.

Now that the parity of the terms of C and S are understood, the correctness of the theorem for the terms involving these is verified similarly to the previous terms.

Appendix B. Detailed calculations for ϵ_2 and for the energy expansion

Appendix B.1. A formula for ϵ_2

For the determination of ϵ_2 we expand the identity (26) in powers up to $O(R^{-2})$. Inserting $\Theta = \Theta_0 + \tilde{\Theta}$, and passing to T as the integration variable, we obtain

$$\int_{-\infty}^{\infty} \left[(\Theta'_0 + \tilde{\Theta}')^2 + \left(1 - \frac{1}{R^2}\right) \sin^2(\Theta_0 + \tilde{\Theta}) \right] dT = 2\pi \left(\epsilon_0 + \frac{\epsilon_2}{R^2} \right) + O(R^{-4}). \quad (\text{B.1})$$

We calculate

$$(\Theta'_0 + \tilde{\Theta}')^2 = \Theta_0'^2 + \frac{1}{R} 2\Theta'_0 \Theta'_1 + \frac{1}{R^2} (2\Theta'_0 \Theta'_2 + \Theta_1'^2) + O(R^{-3}) \quad (\text{B.2})$$

and

$$\begin{aligned} \sin^2(\Theta_0 + \tilde{\Theta}) &= (\sin \tilde{\Theta} \cos \Theta_0 + \cos \tilde{\Theta} \sin \Theta_0)^2 \\ &= \sin^2 \Theta_0 + \frac{1}{R} \Theta_1 \sin 2\Theta_0 + \frac{1}{R^2} (\Theta_1^2 \cos 2\Theta_0 + \Theta_2 \sin 2\Theta_0) + O(R^{-3}). \end{aligned} \quad (\text{B.3})$$

We insert these results into Eq. (B.1). The terms $O(1)$ cancel due to Eq. (28). The $O(R^{-1})$ terms are odd and vanish upon integration. The terms $O(R^{-3})$ vanish for the same reason. The $O(R^{-2})$ terms give

$$\int_{-\infty}^{\infty} (2\Theta'_0 \Theta'_2 + \Theta_2 \sin 2\Theta_0 + \Theta_1'^2 + \Theta_1^2 \cos 2\Theta_0 - \sin^2 \Theta_0) dT = 2\pi \epsilon_2. \quad (\text{B.4})$$

We perform an integration by parts in the first and third terms,

$$\int_{-\infty}^{\infty} [\Theta_2 (\sin 2\Theta_0 - 2\Theta_0') - \Theta_1 (\Theta_1'' - \Theta_1 \cos 2\Theta_0) - \sin^2 \Theta_0] dT = 2\pi \epsilon_2. \quad (\text{B.5})$$

The first parenthesis vanishes due to Eq. (6) and the second one is equal to g_1 due to Eq. (16). We obtain

$$- \int_{-\infty}^{\infty} (\Theta_1 g_1 + \sin^2 \Theta_0) dT = 2\pi \epsilon_2. \quad (\text{B.6})$$

We integrate the second term in the left side by using Eq. (9) and obtain

$$\epsilon_2 = -\frac{1}{\pi} \left(1 + \frac{1}{2} \int_{-\infty}^{\infty} \Theta_1 g_1 dT \right) \quad (\text{B.7})$$

proving a result in Theorem 2. The value of the latter integral is found in Appendix B.3.

Appendix B.2. A formula for the leading order energy

We address the exchange, anisotropy and DM terms under the energy integral (4) separately. The arrows below indicate that only terms $O(R^{-1})$ are taken. They also allow replacement of a term by an equal quantity, omitting terms that integrate to zero, and operations corresponding to integration by parts, for example $\Theta_1'^2$ being replaced by $-\Theta_1'' \Theta_1$.

- Exchange:

$$\begin{aligned} \frac{1}{2}(R+T)\Theta'^2 + \frac{1}{2} \frac{\sin^2 \Theta}{R+T} : &\mapsto \frac{1}{2} \Theta_1'^2 + \Theta_0' \Theta_2' + T \Theta_0' \Theta_1' + \frac{1}{2} \sin^2 \Theta_0 \\ &\mapsto -\frac{1}{2} \Theta_1'' \Theta_1 - \Theta_0'' \Theta_2 - T \Theta_0'' \Theta_1 - \Theta_0' \Theta_1 + \frac{1}{2} \sin^2 \Theta_0. \end{aligned} \quad (\text{B.8})$$

- Anisotropy:

$$\frac{1}{2}(R + T) \sin^2 \Theta : \mapsto \frac{1}{2}\Theta_1^2 \cos 2\Theta_0 + \frac{1}{2}\Theta_2 \sin 2\Theta_0 + \frac{1}{2}T\Theta_1 \sin 2\Theta_0. \quad (\text{B.9})$$

- DM:

$$\begin{aligned} (R + T) \left(\epsilon_0 \Theta' + \frac{\epsilon_2}{R^2} \Theta' \right) + \frac{1}{2} \epsilon_0 \sin 2\Theta : &\mapsto \epsilon_0 \Theta_2' + \epsilon_0 T \Theta_1' + \epsilon_2 \Theta_0' + \epsilon_0 \Theta_1 \cos 2\Theta_0 \\ &\mapsto -\epsilon_0 \Theta_1 + \epsilon_2 \Theta_0' + \epsilon_0 \Theta_1 \cos 2\Theta_0 \\ &\mapsto \epsilon_2 \Theta_0' - 2\epsilon_0 \Theta_1 \sin^2 \Theta_0. \end{aligned} \quad (\text{B.10})$$

The second and third terms in the anisotropy cancel one by one the corresponding exchange terms in view of Eq. (6). The first term in the anisotropy combines with the first term in the exchange to give $-\frac{1}{2}\Theta_1 g_1$ in view of (16). We are left with

$$\begin{aligned} &-\frac{1}{2}\Theta_1 g_1 - (\Theta_0' + 2\epsilon_0 \sin^2 \Theta_0) \Theta_1 + \epsilon_2 \Theta_0' + \frac{1}{2} \sin^2 \Theta_0 \\ &\mapsto \frac{1}{2}\Theta_1 g_1 + \epsilon_2 \Theta_0' + \frac{1}{2} \sin^2 \Theta_0. \end{aligned}$$

We take the integral

$$\int_{-\infty}^{\infty} \left(\frac{1}{2}\Theta_1 g_1 + \epsilon_2 \Theta_0' + \frac{1}{2} \sin^2 \Theta_0 \right) dT = \frac{1}{2} \int_{-\infty}^{\infty} \Theta_1 g_1 dT - \epsilon_2 \pi + 1$$

and use (30) to obtain

$$E_1 = 4\pi \left(1 + \frac{1}{2} \int_{-\infty}^{\infty} \Theta_1 g_1 dT \right) = 4\pi^2 |\epsilon_2|. \quad (\text{B.11})$$

Appendix B.3. Evaluation of the integral in the expressions for ϵ_2 and E_1

We will evaluate the integral appearing in Eqs. (30), (B.7) for ϵ_2 and in Eq. (B.11) for E_1 . For $n = 1$, the solvability condition (21) is equivalent to

$$\int_0^{\infty} g_1(\tau) H_1(\tau) d\tau = 0, \quad (\text{B.12})$$

as a result of the evenness of the integrand. It follows that the lower limit $-\infty$ in Eq. (20) may be replaced with a zero lower limit; the integral in Eq. (30) is then written as

$$\int_{-\infty}^{\infty} \Theta_1 g_1 dT = -\frac{1}{2} \int_{-\infty}^{\infty} dT g_1(T) H_1(T) \int_0^T d\tau g_1(\tau) H_2(\tau) + \frac{1}{2} \int_{-\infty}^{\infty} dT g_1(T) H_2(T) \int_0^T d\tau g_1(\tau) H_1(\tau). \quad (\text{B.13})$$

The two terms on the right in Eq. (B.13) are shown to be equal if we apply integration by parts and use the solvability condition (B.12). We have

$$\int_{-\infty}^{\infty} \Theta_1 g_1 dT = \int_{-\infty}^{\infty} dT g_1(T) H_2(T) \int_0^T d\tau g_1(\tau) H_1(\tau). \quad (\text{B.14})$$

The integral on the right can be calculated explicitly,

$$\int_0^T g_1(\tau) H_1(\tau) d\tau = \tanh T - \frac{2}{\pi} \tanh T \operatorname{sech} T - \frac{4}{\pi} \arctan(e^T) + 1. \quad (\text{B.15})$$

This is inserted into Eq. (B.14) and the integral is evaluated numerically to find

$$\int_{-\infty}^{\infty} \Theta_1 g_1 dT = -0.0790. \quad (\text{B.16})$$

References

- [1] A. N. Bogdanov and D. A. Yablonskii. Thermodynamically stable “vortices” in magnetically ordered crystals. The mixed state of magnets. *Sov. Phys. JETP*, 68:101–103, 1989.
- [2] A. N. Bogdanov and A. Hubert. Thermodynamically stable magnetic vortex states in magnetic crystals. *J. Magn. Magn. Mater.*, 138:255, 1994.
- [3] N. Romming, C. Hanneken, M. Menzel, J. E. Bickel, B. Wolter, K. von Bergmann, A. Kubetzka, and R. Wiesendanger. Writing and deleting single magnetic skyrmions. *Science*, 341(6146):636–639, 2013.
- [4] Pin-Jui Hsu, André Kubetzka, Aurore Finco, Niklas Romming, Kirsten von Bergmann, and Roland Wiesendanger. Electric-field-driven switching of individual magnetic skyrmions. *Nature Nanotechnology*, 12(2):123–126, 2017.
- [5] Sebastian Meyer, Marco Perini, Stephan von Malottki, André Kubetzka, Roland Wiesendanger, Kirsten von Bergmann, and Stefan Heinze. Isolated zero field sub-10 nm skyrmions in ultrathin Co films. *Nature Communications*, 10(1):3823, 2019.
- [6] Arianna Casiraghi, Héctor Corte-León, Mehran Vafaee, Felipe Garcia-Sanchez, Gianfranco Durin, Massimo Pasquale, Gerhard Jakob, Mathias Kläui, and Olga Kazakova. Individual skyrmion manipulation by local magnetic field gradients. *Communications Physics*, 2(1):145, 2019.
- [7] Amandine Aftalion and Peter Mason. Phase diagrams and Thomas-Fermi estimates for spin-orbit-coupled bose-einstein condensates under rotation. *Phys. Rev. A*, 88:023610, Aug 2013.
- [8] Amandine Aftalion and Rémy Rodiac. One dimensional phase transition problem modeling striped spin orbit coupled bose-einstein condensates. *Journal of Differential Equations*, 269:38–81, 2020.
- [9] Paul J. Ackerman, Rahul P. Trivedi, Bohdan Senyuk, Jao van de Lagemaat, and Ivan I. Smalyukh. Two-dimensional skyrmions and other solitonic structures in confinement-frustrated chiral nematics. *Phys. Rev. E*, 90:012505, Jul 2014.
- [10] David C. Wright and N. David Mermin. Crystalline liquids: the blue phases. *Rev. Mod. Phys.*, 61:385–432, Apr 1989.
- [11] C. Melcher. Chiral skyrmions in the plane. *Proc. R. Soc. A*, 470:20140394, October 2014.
- [12] X. Li and C. Melcher. Stability of axisymmetric chiral skyrmions. *J. Funct. Anal.*, 275(10):2817–2844, 2018.
- [13] Anne Bernand-Mantel, Cyrill B Muratov, and Thilo M Simon. A quantitative description of skyrmions in ultrathin ferromagnetic films and rigidity of degree ± 1 harmonic maps from \mathbb{R}^2 to \mathbb{S}^2 . *arXiv preprint arXiv:1912.09854*, 2019.
- [14] Anne Bernand-Mantel, Cyrill B. Muratov, and Thilo M. Simon. Unraveling the role of dipolar versus Dzyaloshinskii-Moriya interactions in stabilizing compact magnetic skyrmions. *Phys. Rev. B*, 101:045416, Jan 2020.
- [15] Carlo Greco. On the existence of skyrmions in planar liquid crystals. *Topological Methods in Nonlinear Analysis*, 2019.
- [16] A O Leonov, T L Monchesky, N Romming, A Kubetzka, A N Bogdanov, and R Wiesendanger. The properties of isolated chiral skyrmions in thin magnetic films. *New Journal of Physics*, 18:065003, 2016.
- [17] H.-B. Braun. Fluctuations and instabilities of ferromagnetic domain-wall pairs in an external magnetic field. *Physical Review B*, 50(22):16485, 1994.
- [18] N. Romming, A. Kubetzka, C. Hanneken, K. von Bergmann, and R. Wiesendanger. Field-dependent size and shape of single magnetic skyrmions. *Phys. Rev. Lett.*, 114:177203, May 2015.
- [19] Y. Zhou, E. Iacocca, A. A. Awad, R. K. Dumas, F. C. Zhang, H.-B. Braun, and J. Åkerman. Dynamically stabilized magnetic skyrmions. *Nature communications*, 6:8193, 2015.
- [20] F. Büttner, I. Lemesh, and S. D. G. Beach. Theory of isolated magnetic skyrmions: From fundamentals to room temperature applications. *Sci. Rep.*, 8:4464, 2018.
- [21] Volodymyr P. Kravchuk, Denis D. Sheka, Ulrich K. Röbber, Jeroen van den Brink, and Yuri Gaididei. Spin eigenmodes of magnetic skyrmions and the problem of the effective skyrmion mass. *Phys. Rev. B*, 97:064403, Feb 2018.
- [22] Olivier Boulle, Jan Vogel, Hongxin Yang, Stefania Pizzini, Dayane de Souza Chaves, Andrea Locatelli, Tevfik Onur Menteş, Alessandro Sala, Liliana D. Buda-Prejbeanu, Olivier Klein, Mohamed Belmeguenai, Yves Roussigné, Andrey Stashkevich, Salim Mourad Chérif, Lucia Aballe, Michael Foerster, Mairbek Chshiev, Stéphane Auffret, Ioan Mihai Miron, and Gilles Gaudin. Room-temperature chiral magnetic skyrmions in ultrathin magnetic nanostructures. *Nat. Nano.*, 11(5):449–454, may 2016.
- [23] D McGrouther, R J Lamb, M Krajnak, S McFadzean, S McVitie, R L Stamps, A O Leonov, A N Bogdanov, and Y Togawa. Internal structure of hexagonal skyrmion lattices in cubic helimagnets. *New Journal of Physics*, 18(9):095004, sep 2016.
- [24] A. Kovács, J. Caron, A. S. Savchenko, N. S. Kiselev, K. Shibata, Zi-An Li, N. Kanazawa, Y. Tokura, S. Blügel, and R. E. Dunin-Borkowski. Mapping the magnetization fine structure of a lattice of Bloch-type skyrmions in an FeGe thin film. *Applied Physics Letters*, 111(19):192410, 2017.
- [25] K. Shibata, A. Kovács, N. S. Kiselev, N. Kanazawa, R. E. Dunin-Borkowski, and Y. Tokura. Temperature and magnetic field dependence of the internal and lattice structures of skyrmions by off-axis electron holography. *Physical Review Letters*, 118(8):087202, 2017.
- [26] Sebastian Meyer, Marco Perini, Stephan von Malottki, André Kubetzka, Roland Wiesendanger, Kirsten von Bergmann, and Stefan Heinze. Isolated zero field sub-10 nm skyrmions in ultrathin Co films. *Nat. Comm.*, 10:3823, Aug 2019.

- [27] Karin Everschor-Sitte, J. Masell, R. M. Reeve, and M. Kläui. Perspective: Magnetic skyrmions—overview of recent progress in an active research field. *J. Appl. Phys.*, 124:240901, 2018.
- [28] C. Schütte and M. Garst. Magnon-skyrmion scattering in chiral magnets. *Phys. Rev. B*, 90:094423, Sep 2014.
- [29] Volodymyr P. Kravchuk, Olena Gomonay, Denis D. Sheka, Davi R. Rodrigues, Karin Everschor-Sitte, Jairo Sinova, Jeroen van den Brink, and Yuri Gaididei. Spin eigenexcitations of an antiferromagnetic skyrmion. *Phys. Rev. B*, 99:184429, May 2019.
- [30] Stavros Komineas, Christof Melcher, and Stephanos Venakides. The profile of chiral skyrmions of small radius. *arXiv*, page 1904.01408, 2019.
- [31] I. V. Baryakhtar and B. A. Ivanov. Nonlinear vortex excitations (solitons) in a 2d magnetic materials of the YBaCuO type. *JETP Lett.*, 55:624, 1992.
- [32] L. D. Landau and E. M. Lifshitz. *Quantum Mechanics*. Pergamon Press, Oxford, second edition, 1965.
- [33] S. Novikov, S. V. Manakov, L. P. Pitaevskii, and V. E. Zhakharov. *Theory of solitons*. Plenum Publishing Corporation, New York, 1984.
- [34] S. Rohart and A. Thiaville. Skyrmion confinement in ultrathin film nanostructures in the presence of Dzyaloshinskii-Moriya interaction. *Phys. Rev. B*, 88:184422, Nov 2013.
- [35] V. P. Voronov, B. A. Ivanov, and A. M. Kosevich. Two-dimensional dynamic topological solitons in ferromagnets. *Sov. Phys. JETP*, 57:1303, 1983.
- [36] Milton Abramowitz and Irene A. Stegun. *Handbook of Mathematical Functions with Formulas, Graphs, and Mathematical Tables*. Dover, New York, ninth Dover printing, tenth GPO printing edition, 1964.
- [37] The Sage Developers. *SageMath, the Sage Mathematics Software System (Version 8.7)*, 2019. <https://www.sagemath.org>.
- [38] G. H. Derrick. Comments on nonlinear wave equations as models for elementary particles. *J. Math. Phys.*, 5:1252, 1964.
- [39] Hongying Jia, Bernd Zimmermann, Markus Hoffmann, Moritz Sallermann, Gustav Bihlmayer, and Stefan Blügel. Material systems for fm-/afm-coupled skyrmions in co/pt-based multilayers, 2020.
- [40] Stavros Komineas and Nikos Papanicolaou. Traveling skyrmion in chiral antiferromagnets. *SciPost Phys.*, 8:086, 2020.